Energy Conversion and Management 60 (2012) 36–44

Contents lists available at SciVerse ScienceDirect

Energy Conversion and Management

journal homepage: www.elsevier.com/locate/enconman

Integrated system approach for increase of engine combined cycle efficiency

D. Gewald [a,*], S. Karellas [b], A. Schuster [a], H. Spliethoff [a]

[a] Institute for Energy Systems, Technische Universität München, Boltzmannstr. 15, 85748 Garching, Germany
[b] Laboratory of Steam Boilers and Thermal Power Plants, National Technical University of Athens, Heroon Polytechniou 9, 15780 Athens, Greece

ARTICLE INFO

Article history:
Available online 20 March 2012

Keywords:
Internal combustion engine (ICEs)
Waste heat recovery
Water/steam-cycle
Optimization

ABSTRACT

Internal combustion engines (ICEs) are widely used as independent power producers due to their high electrical efficiency (up to 47%), which can be further enhanced by operating them in combined cycle mode with a water/steam cycle as bottoming cycle.

This study presents an integrated approach to optimize the combined cycle overall system efficiency. Therefore, not only the most favorable design of the waste heat recovery (WHR) cycle, but also the optimal configuration of the ICE cooling system have to be investigated, in order to integrate both available engine waste heat sources (exhaust gas, 300–400 °C, engine cooling water, 90 °C) into the waste heat recovery cycle. For the definition of the most favourable temperature level of the engine cooling water three variants of engine cooling systems are examined, with respect to technical limitations given by the ICE. In order to determine the types of engines for which this optimization approach is suitable, three types of engines with different characteristics (fuel, exhaust gas parameters) combined with a water/steam cycle are simulated, by using the calculation tools Excel and Ebsilon Professional. An energetic, exergetic and economic analysis is conducted. These reveal the impacts of the temperature level to the WHR system and to the design of the engine cooling system. The calculations performed, showed that up to 19% of the engine cooling water heat can be efficiently recovered compared to a portion of 6% in the standard system. The better recovery leads to a 5%-decrease in the costs of electricity generation.

1. Introduction

Due to their high electrical efficiency (up to 47%) in stationary operation, internal combustion engines (ICE) are widely used as independent power producers. They form a valuable solution for the power production in remote areas [1,2], given also their ability to run on different fuels, e.g. heavy fuel oil (HFO), gaseous fuels or bio-fuels, with the latter ones drawing recently world-wide attention due to their renewable character. These include works for example reported in [3] for the spray development with vegetable oil, biodiesel or diesel fuels in high-speed diesel engine, in [4] for the emissions and noise of turbocharged diesel engine during starting using bio-diesel or *n*-butanol diesel fuel blends, in [5] for the performance and exhaust emissions of heavy duty (bus) diesel engine using ethanol–diesel fuel blends, in [6] for combustion heat release analysis and emissions in high-speed diesel engine using neat cottonseed oil or its neat bio-diesel, and in [7] for combustion heat release analysis and emissions of ethanol or *n*-butanol diesel fuel blends in heavy-duty diesel engine.

However, about 45% of fuel energy is converted into high- and low-temperature heat in the exhaust gas and the engine cooling water. Therefore, waste heat recovery (WHR) for power generation is a striking measure both to improve electrical efficiency and to decrease the environmental influence of an ICE. Therefore also engine manufacturers are already doing research on this technology [8,9] or even implementing it in ICE power plants [10].

Hence, many studies on the implementation of a WHR system for ICEs have been conducted in literature. These studies are usually focussing on the optimization of the "after-engine-construction", which is the selection and comparison of suitable WHR systems, e.g. [11,9] are focusing on the implementation and optimization of water/steam cycles as WHR systems, [12] is evaluating different Organic-Rankine-Cycle (ORC) configurations as ICE bottoming cycles, while [13] is comparing the ORC and the Kalina cycle and [14] the water/steam and the ORC. Refs. [15,16] are comparing different WHR cycle alternatives including mechanical and electrical turbo-compounding. Among those, only a few studies can be found, where both engine heat sources are used as input to a single WHR system [14,17].

Regarding the optimization of the whole system, that is ICE together with WHR, only Holmes and Lucas [17] is describing the optimization of engine design and construction parameters in order to not only increase the engine but the overall system efficiency of electric power generation. The literature survey shows as well, that just a small amount of the engine cooling water heat

* Corresponding author.
E-mail address: daniela.gewald@tum.de (D. Gewald).

0196-8904/$ - see front matter © 2012 Elsevier Ltd. All rights reserved.
doi:10.1016/j.enconman.2011.10.029

can be integrated in a WHR system with the input of both heat sources. This amount is usually around 6% for a standard engine cooling system [18].

Thus, efforts on the better integration of low temperature waste heat are missing in the current literature. The engine cooling systems and the possible changes in those systems, which lead to a higher portion of integrated low temperature heat, have to be examined. Therefore this paper is presenting an integrated approach of combined cycle optimization. Firstly three different engines and their cooling systems are described, followed by the thermodynamic evaluation of changes in the cooling systems. In order to estimate the cost effectiveness of higher cooling water integration, all measures are also evaluated economically by calculating their costs of electricity generation.

2. Cycle modelling

In this section the standard cooling system of an ICE and the thermodynamic modelling of the bottoming cycle will be described. The MAN 18V 48/60, MAN 20V 35/44 SI and Jenbacher 620 GS engines will be taken as examples. These are typical engines for stationary power generation fired by heavy fuel oil and natural gas. The most important engine parameters are given in Table 1. Moreover, the waste heat potential for a bottoming cycle will be calculated and the methods for cycle efficiency and heat exchanger area calculation are presented.

2.1. ICE cooling system and waste heat potential

In an ICE several components have to be cooled. Considering the temperature levels of the different coolers, two different cooling cycles are applied to the ICE:

Table 1
Important engine parameters.

	18V 48/60	20V 35/44	J620 GS
Fuel	HFO	Natural gas	Natural gas
P_{mech} (kW)	18,900	10,600	3120
Exhaust gas:			
T_{ex} (°C)	360	298	425
$\dot{m}_{ex}$ (kg/s)	34.7	18.5	4.8
Temperature restriction at HRSG outlet (°C)	160	None	None
HT cooling water:			
T_{HT} (°C)	90	93	90
$\dot{m}_{HT}$ (kg/s)	54.6	38.3	16.6

- The low temperature (LT) cycle is cooling the second stage of the charge air, the nozzles, (and lube oil in case of MAN engines). The temperature level of this cycle is depending on ambient conditions and is usually between 40 and 60 °C.
- The high temperature (HT) cycle is cooling the cylinders, the first stage of the charge air (and lube oil in case of Jenbacher engine). Its temperature level is controlled, such that the outlet temperature of the cylinder cooler is 90 °C and 80 °C respectively.

A scheme of the standard MAN 18V 48/60 cooling system with an integrated heat consumer is shown in Fig. 1.

The cooling system of the MAN 20V 35/44 is an exception because the CAC I and the cylinder cooler are interchanged in that system with a corresponding temperature level of 92.9 °C before the heat consumer. The interchanged system will be discussed in Section 3.2 of this paper.

Since the temperature level of the LT cooling cycle is even too low for the condensate preheating of the bottoming cycle in most cases, changes in the LT cycle will not be considered in the following sections. The temperature level of 90 °C/80 °C in the HT system behind the cylinder cooler is a boundary condition given by the ICE, which cannot be changed. This has to be considered in the optimization process of the cooling system.

A typical heat flow diagram for medium speed ICEs is shown in Fig. 2. Fig. 3 shows the waste heat potential of the engine HT cooling cycle for the three exemplary engines.

2.2. Modelling of the bottoming cycle

As bottoming cycle, a water/steam process is considered. A schematic of this process is given in Fig. 4 for a diesel (a) and a gas engine (b) respectively.

The exhaust gases are recovered in a natural circulation heat recovery steam generator (HRSG). With the low grade heat of the exhaust gases saturated steam is produced for the deaeration. The steam is used both for heating the feedwater tank and for producing saturated steam in the feedwater tank. This steam is fed to the low pressure stage of the turbine. The condensate is preheated by HT cooling water in the condensate preheater I. In the case of engines, which exhaust gases can be cooled down without any temperature restriction (given by example to prevent condensation of sulphuric acid, see Table 1), a second condensate preheater II is installed within the exhaust gas flow. Especially for HFO engines some of the saturated steam is taken from the steam drum for auxiliary purposes. This steam is used for fuel preheating at different temperature levels. To simplify calculations, the steam own consumption of the engine is neglected in further sections.

Important parameters like live steam and condensate pressures are chosen according to the exhaust gas parameters and the ambient conditions.

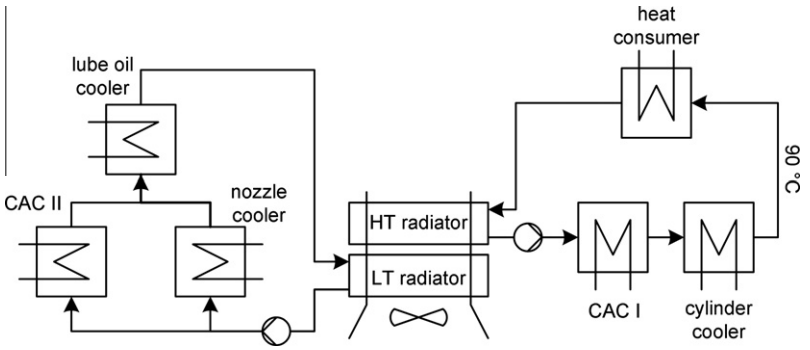

Fig. 1. Scheme of the MAN 18V 48/60 standard cooling system.

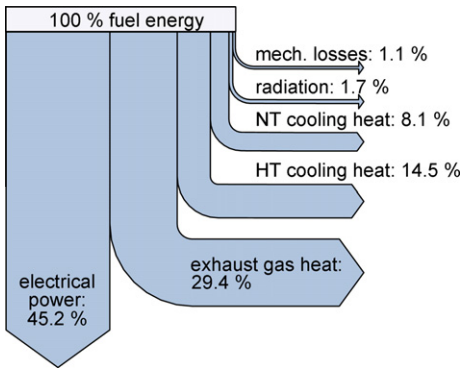

Fig. 2. Typical energy flow diagram for medium speed ICEs.

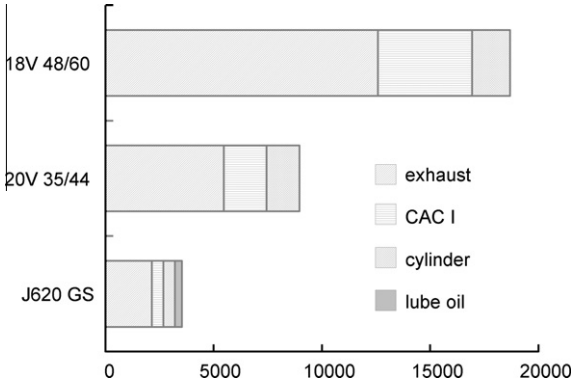

Fig. 3. Engine waste heat potential.

The water-steam-cycle is calculated using the REFPROP formulation of NIST [19] for water and steam properties within an Excel file. The engine cooling water cycle is simulated by using the software Ebsilon 9.0 [20] for thermodynamic cycle calculations.

2.3. Energy and exergy calculation

The thermodynamic efficiency η_{th} is calculated by means of the first law of thermodynamics [21]:

$$\eta_{th} = \frac{P_{el,net}}{\dot{Q}_{input}} \tag{1}$$

with

$$P_{el,net} = (P_{th,turbine} - P_{own\ consumption}) \cdot \eta_{mech} \cdot \eta_{gen} \tag{2}$$

$$\dot{Q}_{input} = \dot{Q}_{exhaust} + \dot{Q}_{HT\ cooling} \tag{3}$$

To calculate the thermodynamic and the exergetic efficiency respectively, the following component, mechanical and electrical efficiencies (see Table 2) were used in all WHR system calculations:

The exergetic efficiency of the cycle and the components is evaluated according to the second law of thermodynamics. Formulations for the cycle exergetic efficiency are given below [21]:

$$\eta_{ex} = \frac{P_{el,net}}{\dot{E}_{input}} \tag{4}$$

$$\dot{E}_{input} = \dot{E}_{exhaust} + \dot{E}_{HT\ cooling} \tag{5}$$

$$\dot{E}_{ex/HT} = \dot{m}_{ex/HT} \cdot [h_{in} - h_0 - T_0 \cdot (s_{in} - s_0)] \tag{6}$$

Formulations for component efficiency are given by Nikulshin et al. [22] and Mago, Charma [23]:

- heat exchanger:

$$\eta_{ex,HE} = \frac{\dot{E}_{c,out} - \dot{E}_{c,in}}{\dot{E}_{h,in} - \dot{E}_{h,out}} \tag{7}$$

- turbine:

$$\eta_{ex,T} = \frac{P_{el,T}}{\dot{E}_{s,in} - \dot{E}_{s,out}} \tag{8}$$

- pump:

$$\eta_{ex,P} = \frac{\dot{E}_{w,out} - \dot{E}_{w,in}}{P_{el,P}} \tag{9}$$

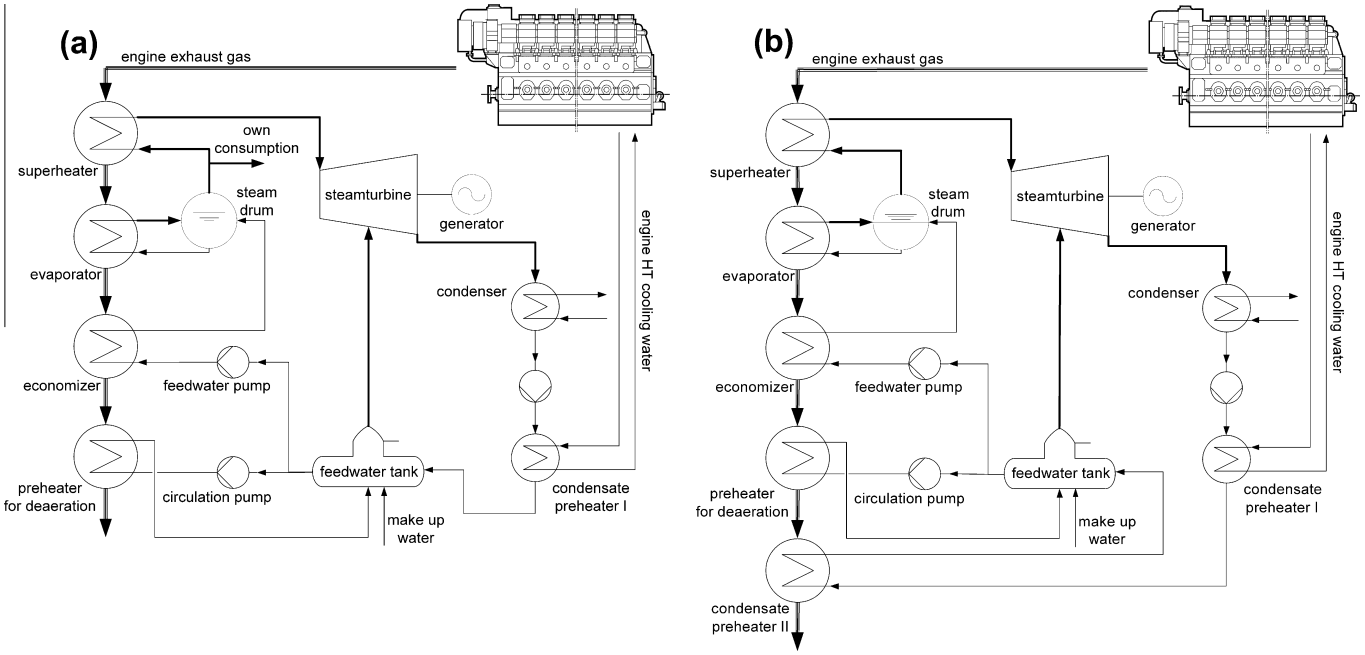

Fig. 4. Steam bottoming cycle for (a) HFO engines and (b) natural gas engines.

Table 2
Efficiencies for WHR calculations.

Isentropic steam turbine efficiency	$\eta_{is,turbine}$	75%
Isentropic pump efficiency	$\eta_{is,pump}$	80%
Mechanical efficiency	η_{mech}	98%
Generator efficiency	η_{gen}	98%

2.4. Heat exchanger area calculation

Several heat exchangers of different types are used within the engine cooling system and for the heat transfer from the cooling system to the bottoming cycle. In order to estimate the economic effect of the thermodynamic cycle optimization, the areas of the heat exchangers, which are mostly affected by the cycle optimization, have to be calculated. The calculation methods for the heat exchangers are described in this section. All equations used are given in different sections of the VDI Heat Atlas [24].

2.4.1. Plate heat exchangers

The heat of the HT cooling cycle is transferred to the bottoming steam cycle via plate heat exchangers. The following correlations can be used to determine the area of a technical plate heat exchanger with single phase water flow:

$$Nu = c_q Pr^{1/3} \left(\frac{\eta}{\eta_w}\right)^{1/6} [\xi Re^2 sin(2\pi)] \tag{10}$$

with $c_q = 0.122$ and $q = 0.374$ and

$$\xi Re^2 = \frac{2\Delta p d_h^3 \rho}{L_p \eta^2} \tag{11}$$

the hydraulic diameter of plate heat exchangers is calculated as following:

$$d_h = \frac{4\hat{a}}{\Phi} \tag{12}$$

$$\Phi(X) \approx \frac{1}{6}\left(1 + \sqrt{1+X^2} + 4\sqrt{1+\frac{X^2}{2}}\right) \tag{13}$$

$$X = \frac{2\pi\hat{a}}{\Lambda} \tag{14}$$

2.4.2. Radiator and charge air coolers

The radiator and charge air coolers consist of bundels of staggered, finned pipes. For staggered finned pipes the air side heat transfer coefficient α_S can be determined by calculating the air side heat transfer coefficient for plain pipes α_R (16), using a Nusselt-correlation (17), and the fin efficiency η_R (18):

$$\alpha_S = \alpha_R \left[1 - (1-\eta_R)\frac{A_R}{A}\right] \tag{15}$$

$$\alpha_R = \frac{Nu \cdot \lambda_{air}}{d} \tag{16}$$

$$Nu = 0.38 \cdot Re^{0.6} \cdot \left(\frac{A}{A_{G_0}}\right)^{-0.15} \cdot Pr^{1/3} \tag{17}$$

$$\eta_R = \frac{tanhX}{X} \tag{18}$$

$$X = \phi \frac{d}{2}\sqrt{\frac{2\alpha_R}{\alpha_R \cdot s}} \tag{19}$$

$$\phi = \left(\frac{D}{d} - 1\right)\left[1 + 0.35 ln\left(\frac{D}{d}\right)\right] \tag{20}$$

The water side heat transfer coefficient can be estimated by using the equation of Dittus–Bölter [25]:

$$Nu = 0.024 \cdot Re^{0.8} \cdot Pr^{1/3} \cdot \left(1 + \frac{d_h}{l}\right)^{2/3} \tag{21}$$

For the area calculation of charge air coolers, a software tool by GEA (manufacturer of charge air coolers) [26] is used. This tool is also based on the calculation method of staggered finned pipes, described by the Eqs. (15)–(20), and the Dittus–Bölter correlation (21).

2.5. Conditions and restrictions

In order to achieve comparable results of calculations, the same boundary and ambient conditions are used. For ambient conditions the thermochemical reference state [21] will be used:

- air temperature: 25 °C
- air pressure: 1.0 bar

Changes in the cooling system mostly affect the design of the charge air coolers (CAC). Different types of CACs are used with different engines. To avoid a completely new design of the CACs (which would heavily affect the engine construction), the optimal cycle configuration should be defined within the boundary conditions given by the CAC. These are:

- water velocity: 0.5–3.0 m/s
- engine cooling water volume flow: ±10% of nominal flow
- maximum water pressure loss: 0.5 bar in each stage of the CAC
- maximum air pressure loss: 1% of charge air pressure
- some constructive boundary conditions regarding the size of the CACs

Furthermore, all systems are calculated under steady-state conditions and pressure and heat losses in pipes and heat exchangers are neglected.

3. Thermodynamic cycle optimization

Firstly, the characteristic numbers of the basic cycle with the standard cooling system will be presented, to give a basis for the optimization approaches. Subsequently, two different changes in the cooling water system will be evaluated in this section:

- interchanging the cylinder and the first stage CA cooler
- dividing the first stage CA cooler into two parts

3.1. Basic cycle

Fig. 5 shows an energy and exergy flow chart of the basic cycle of the MAN 18V48/60 engine. The data is calculated on the basis of the heat input to the bottoming cycle: the exhaust heat together with the HT cooler heat is 100% heat input (bold figures). The same is valid for the exergy calculation.

Those calculations were also conducted for the 20V 35/44 and the J620 GS engine. The key figures for all three engine bottoming cycles are given in Table 3.

3.2. Interchange of HT and cylinder cooler

The integration of HT heat in the bottoming cycle can only be improved by increasing the HT temperature. Since the outlet temperature of the engine cooler is restricted to 90 °C (for MAN 18V 48/60 and Jenbacher J620 GS engine), the simplest way to increase the HT temperature is to interchange the engine and the first stage CA cooler (see Fig. 6).

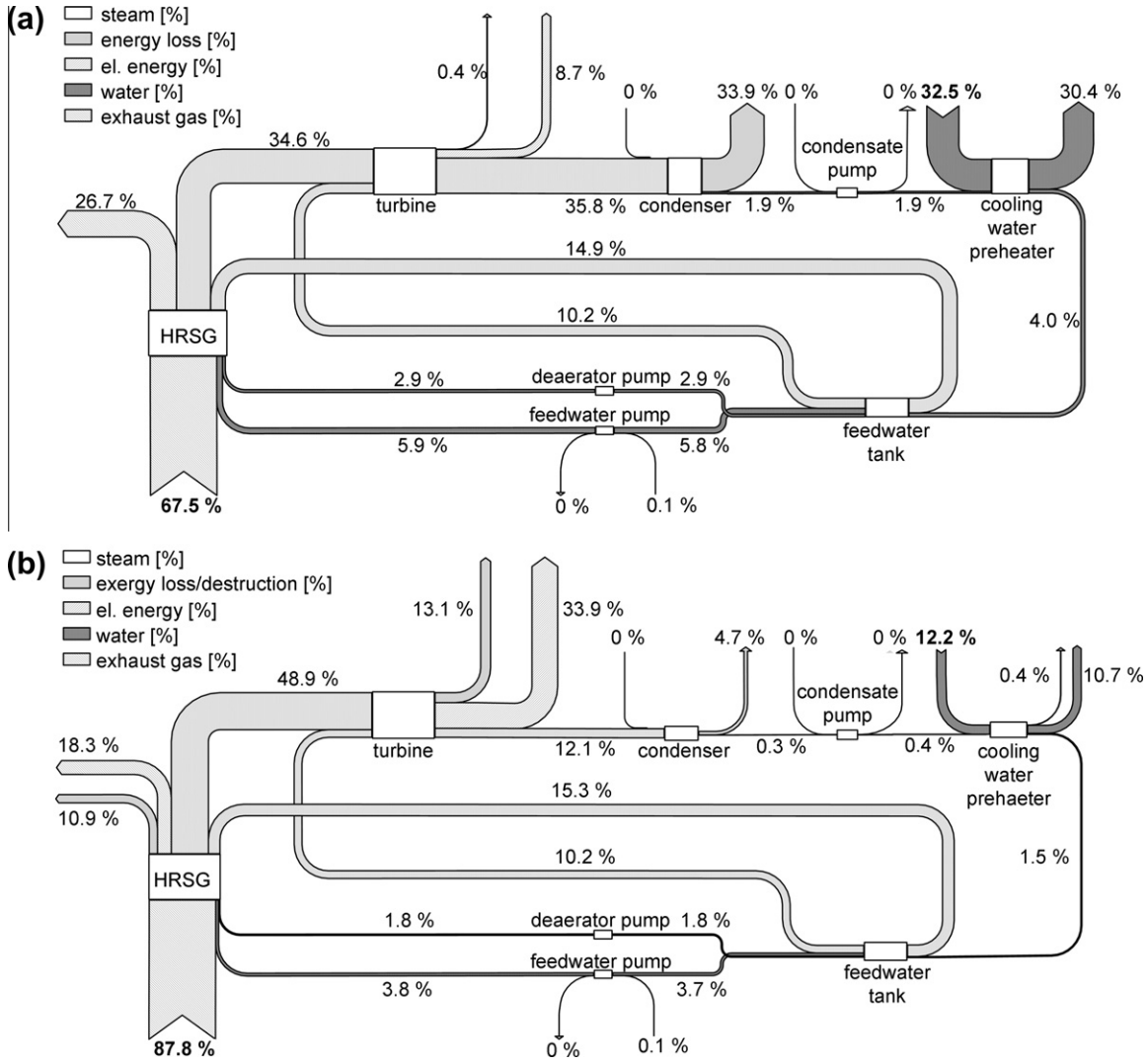

Fig. 5. (a) Sankey chart and (b) Grassmann chart of the 18V 48/60 bottoming cycle.

Table 3
Important data of the standard engine cycles.

	18V 48/60 (%)	2V 35/44 SI (%)	J620 GS (%)
El. efficiency of engine	45.2	46.5	44.1
El. efficiency of systems	49.2	49.1	47.8
Bottoming cycle efficiencies:			
El. efficiency (net)	8.7	6.4	9.7
Ex. efficiency (net)	33.9	29.5	36.9
Transferred exhaust heat	60.5	63.1	76.8
Transferred HT heat	6.5	6.0	6.0

With that measure, the temperature level of the HT cooling cycle is increased above 100 °C (depending on the engine).

3.3. Three stage cooling

Since the mass flow through the cylinder cooler is restricted and thus the HT outlet temperature cannot be increased above ca. 106 °C, the split of the charge air cooler in two parts (CAC Ia and CAC Ib) within the HT cycle will be discussed in this section.

As it can be seen from the scheme in Fig. 7, this cooling system becomes more complicated. An emergency cooler is needed in the cycle of the CAC Ia. The emergency cooler is operated by HT cooling water in the case that the heat consumer in the cycle is not working. The heat of the CAC Ia is also rejected to the environment by the HT radiator. An additional radiator stage is not necessary. Due to a temperature level of approximately 145 °C in the CAC Ia system, the operational pressure has to be raised from 4 bar to 6 bar.

The additional equipment (emergency cooler, pump and valves) as well as the additional costs due to the higher pressure level will negatively influence the installation costs of the engine cooling system. This influence will be evaluated economically in Section 4.

3.4. Comparison of thermodynamic results

3.4.1. 18V 48/60

The optimization results show, that the HT heat recovery can be improved from 6.5% to 12.0% and 17.1% for the interchanged cooling system and the three-stage cooling, respectively (cf. Fig. 8). These figures refer to the effective heat input of the bottoming cycle, which is different for each cooling system since the quantities of heat are shifted within the HT and the LT cycle with differing temperatures of the HT cycle. When the heat recovery is calculated referring to the amount of heat, which is available in the standard system, the heat recovery is improved up to 18.9% with the three stage cooling.

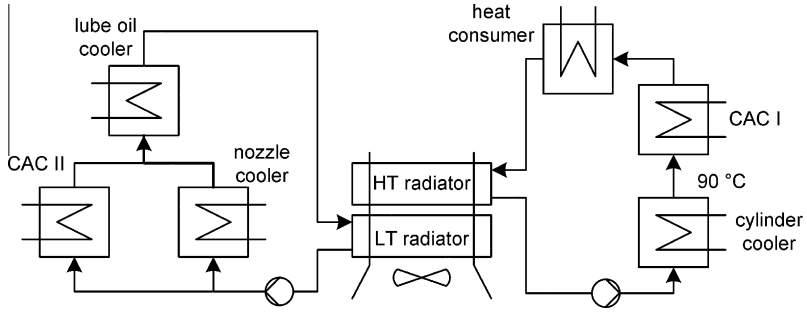

Fig. 6. Engine cooling system with interchanged coolers.

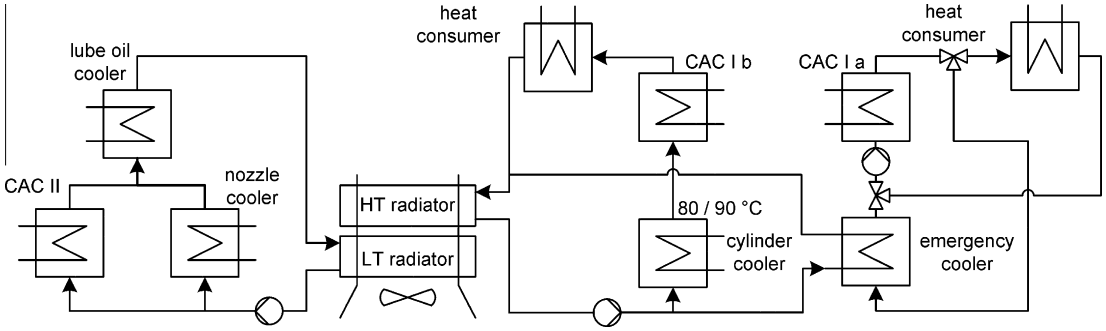

Fig. 7. Three stage engine cooling system.

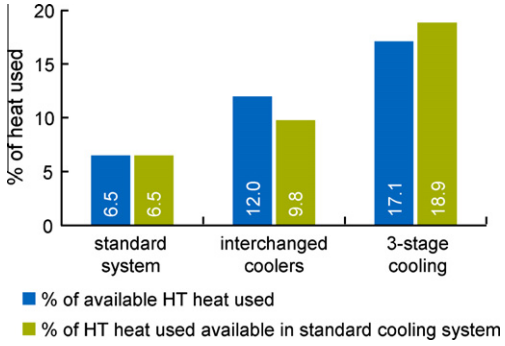

Fig. 8. Improvement of HT energy recovery by cooling system optimization of 18V 48/60.

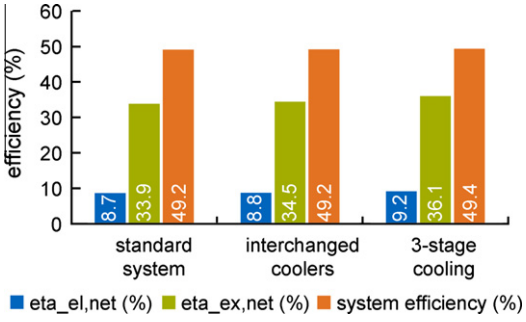

Fig. 9. Key figures of the 18V 48/60 steam bottoming cycle referring to heat and exergy input of the standard system.

The electrical and exergetic efficiencies of the bottoming cycle and the electrical efficiency of the system was calculated. Fig. 9 shows these figures referring to the amount of heat and exergy available in the standard cycle. For the interchanged system, the electrical and exergetic efficiency increase from 8.7% to 8.8% and from 33.9% to 34.5%, respectively, while the system efficiency stays almost the same at 49.2%. With the three-stage cooling, the electrical efficiency increases by further 0.5%-points to 9.2%, compared to the standard system. The exergetic efficiency increases as well to 36.1%, while the system efficiency can be slightly increased to 49.4%.

3.4.2. 20V 35/44

As already mentioned in Section 2.1, the standard cooling system for this engine is the interchanged system. Therefore, only the results for the three-stage cooling in comparison to the interchanged system will be presented.

Figs. 10 and 11 show that the recovery of HT heat can increase from 6.0% to 10.3% and 10.4% respectively. The electrical efficiency of the bottoming cycle and the system stays the same at 6.4% and 49.1% respectively and the exergy efficiency is decreasing from 29.5% to 27.8%. The decrease of exergy efficiency can be explained by the higher exergy input of the cooling water, which cannot be effectively used by the steam system. On the other hand the exergy losses caused by the exhaust gas become higher for the three-stage cooling. Since there is no temperature restriction for the exhaust gases at the HRSG outlet for gas engines, the turbine condensate is first preheated by the HT cooling water and afterwards by the exhaust gases (see Fig. 4b). When the temperature level of the condensate after condensate preheater I is higher, the heat recovery in condensate preheater II is lower. Therefore, the exhaust gas outlet temperature is higher as well. This causes a smaller degree of exhaust gas energy recovery within the HRSG – 60.2% of exhaust gas heat compared to 63.1% and higher exergy losses (see Fig. 12).

3.4.3. J620 GS

The different cooling water system configurations were not separately calculated for the Jenbacher J620 GS engine, since the same phenomenons of lower exergy efficiency and higher exergy losses

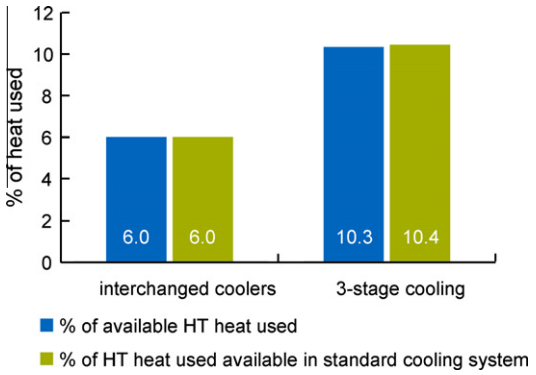

Fig. 10. Improvement of HT energy recovery by cooling system optimization of 20V 35/44.

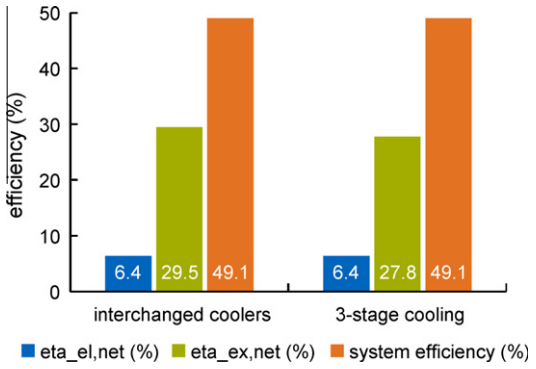

Fig. 11. Key figures of the 20V 35/44 steam bottoming cycle referring to heat and exergy input of the standard system.

in HRSG with increasing cooling water temperatures occur. Changes in the cooling water system do not affect the system power output and thus an optimization process is useless.

4. Economic evaluation of optimized results

Section 3.4 shows that the thermodynamic optimization is effective only for the MAN 18V 48/60 engine. Consequently, the economic analysis will be conducted just for that engine. To evaluate the different cooling water cycles, the costs of electricity generation of each system will be calculated according to the annuity method by VDI 2067 [27]. Some calculation principles for the static annuity method are described.

Costs are subdivided into three categories:

- capital-related
- consumption- and requirement related
- operation related

For the calculations, only the investment costs of the WHR systems are considered (capital related costs), since additional fuel is not needed and operation related costs and the capital related costs of the engine cycle are not affected by the changes in the cooling water system: The annuities of capital-related and operation-related costs are calculated with the equations given by VDI 2067, as follows:

Annuity factor a: required to allocate singular payments (e.g. the investment costs A_0) to yearly amounts that are all equal throughout the period of observation T.

$$a = \frac{(q+1)^T \cdot q}{(q+1)^T - 1} \tag{22}$$

Annuity of capital related costs A_c: the equalized yearly payment, that is calculated with the annuity factor a, the investment costs A_0, the costs for replacement purchases of components $A_1 \ldots A_n$ and the residual value R of these components.

$$A_c = (A_0 + A_1 + A_2 + \cdots + A_n - R) \cdot a \tag{23}$$

$$A_i = \frac{A_0}{(q+1)^{i \cdot T_l}}; \quad i = 1 \ldots n \tag{24}$$

$$R = A_0 \cdot \frac{T_l - T}{T_l \cdot (1+q)^T} \tag{25}$$

The specific costs of electricity production are then calculated by:

$$c_{EP} = \frac{A_c + A_{op}}{P_{net} \cdot T_{full\,load}} \tag{26}$$

As engine combined cycle power plants are mostly working in base load operation, the full load hours $T_{full\,load}$ will be assumed with 7000 h. The calculations are based on a power plant with five 18V 48/60 engines, which has a power output of about 100 MWel.

For the interchanged cooling system, no additional costs are expected compared to the standard system, since neither additional components nor stronger materials are needed. Therefore, the investment costs for the whole WHR system with interchanged coolers are the same as for the standard system. In the case of the three-stage cooling, an emergency cooler and a second heat exchanger for the heat consumer has to be installed.

According to the formulations given above, the costs of electricity generation were calculated for the different systems with the assumptions given in Table 4:

The investment costs A_0 were partly derived from a large data base of offers from component manufacturers for WHR systems.

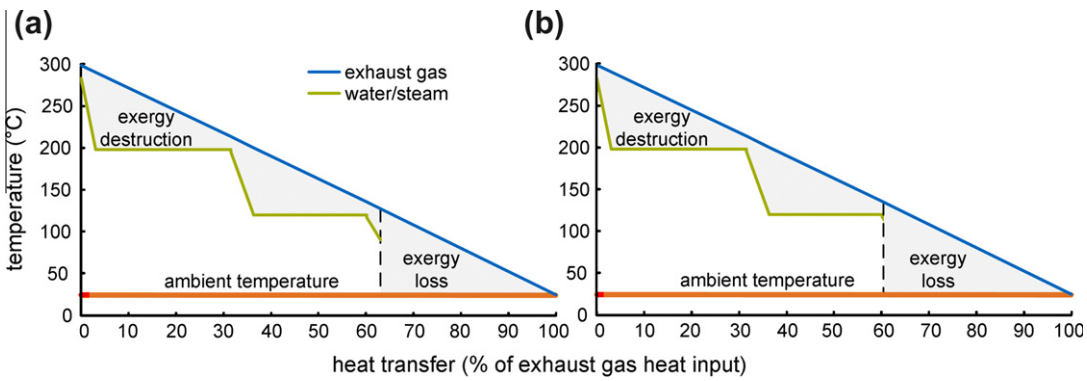

Fig. 12. Exergy destruction and exergy loss in HRSG for (a) interchanged cooling system and (b) three-stage cooling system.

Table 4
Key figures for the economic calculations.

Calculation parameter		Key figure
Period of observation	T	20 years
Lifetime of components	T_l	20 years
Interest factor	q	1.1
Factor for repair and maintenance in order to calculate A_{op}	f_{op}	3.5% (of A_0)

Table 5
Specific costs of invest for the WHR systems.

System	Specific invest ($A_0/P_{el,net}$) (€/kW)
WHR with standard system	1085
WHR with interchanged system	1065
WHR with three-stage cooling	1025

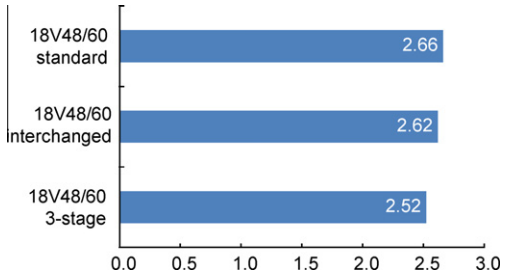

Fig. 13. Costs of electricity production for different WHR systems of the 18V 48/60 engine.

This concerns mainly the costs of the steam generation system and the steam turbine. The costs of the heat exchangers, which are necessary for the integration of cooling water heat into the bottoming cycle, and of the charge air coolers, are based on the area calculation of those heat exchangers according to Section 2.4 and on key figures for heat exchanger areas prices. Table 5 gives an overview of the specific investment costs of the three systems.

Fig. 13 shows that the costs of electricity production differ just slightly for the different WHR systems. For the three-stage system they are reduced to about 95% of the costs of the standard system.

5. Conclusion and outlook

The most important result of the calculations is that – regarding the production of electricity – the use of cooling water heat at higher temperature levels is useful only for engines, which have a restriction in the exhaust gas outlet temperature at the HRSG (e.g. HFO fired engines). For those engines, it is possible to increase the power output of the WHR systems by 0.5%-points and to reduce the costs of electricity production by 5% with the integrated system approach.

When exhaust gases can be cooled without any restriction (e.g. engines fired with natural gas), the use of cooling water at heat above 90 °C is counterproductive with respect to exergy efficiency, since a higher amount of exhaust gas exergy will be dissipated to the environment.

However, efforts to increase the temperature level of HT heat might still be useful even for gas engines, if CHP applications are taken into account. Electric power is provided by the engine, while heat is produced by exhaust gas and cooling water. For typical district heating applications with forward temperatures of 130 °C and return temperatures of 70 °C, additional calculations have shown, that an HT temperature of more than 100 °C improves the CHP performance and the fuel efficiency (82% in case of the 20V 35/44 engine). Higher cooling water temperatures are also desirable for combined power, heat and cooling applications with absorption refrigeration units [28].

As stated in Section 2, all systems were calculated under steady state conditions. However, ICEs often have to operate under transient conditions. When using a WHR system with integrated use of the engine cooling water, the WHR system is coupled to the engine twice – to the exhaust gas and the cooling water, and therefore dealing with alternating loads. Thus, further studies have to examine the behaviour of the combined system and the mutual influence of ICE and WHR under transient conditions [29,30]. When using an Organic Rankine Cycle instead of a water/steam cycle, the optimal temperature levels and even the way of integration of the cooling water to the WHR cycle might be different according to the different organic working fluids (e.g. R245fa, pentane, MDM) with different thermodynamic characteristics [31,32]. The temperature levels and the potential of integration have to be defined individually for every fluid, which could be the scope of further studies.

References

[1] Pischinger R, Klell M, Sams T. Thermodynamik der Verbrennungskraftmaschine. Berlin/Heidelberg: Springer; 2009.
[2] Dommermuth C, Lenz P, Pointner PL, Garcon S. Image study diesel power plants. Augsburg: MAN Diesel & Turbo; 2010.
[3] Rakopoulos CD, Antonopoulos KA, Rakopoulos DC. Multi-zone modeling of Diesel engine fuel spray development with vegetable oil, bio-diesel or Diesel fuels. Energy Convers Manage 2006;47:1550–73.
[4] Rakopoulos CD, Dimaratos AM, Giakoumis EG, Rakopoulos DC. Study of turbocharged diesel engine operation, pollutant emissions and combustion noise radiation during starting with bio-diesel or *n*-butanol diesel fuel blends. Appl Energy 2011;88:3905–16.
[5] Rakopoulos DC, Rakopoulos CD, Kakaras EC, Giakoumis EG. Effects of ethanol–diesel fuel blends on the performance and exhaust emissions of heavy duty DI diesel engine. Energy Convers Manage 2008;49:3155–62.
[6] Rakopoulos CD, Rakopoulos DC, Giakoumis EG, Dimaratos AM. Investigation of the combustion of neat cottonseed oil or its neat bio-diesel in a HSDI diesel engine by experimental heat release and statistical analyses. Fuel 2010;89:3814–26.
[7] Rakopoulos DC, Rakopoulos CD, Papagiannakis RG, Kyritsis DC. Combustion heat release analysis of ethanol or *n*-butanol diesel fuel blends in heavy-duty DI diesel engine. Fuel 2011;90:1855–67.
[8] Gewald D, Böckhoff N, König N, Spliethoff H. The MAN diesel combined cycle and its influence on the Carbon Footprint. In: Power Gen Europe 2010, Amsterdam.
[9] Kunberger K. Combined-cycle diesel power. Diesel Gas Turbine Worldwide 1998;30:62–7.
[10] Kakakhel I. PM to inaugurate 225 MW Atlas power plant in Sheikhupura today; 2009.
[11] Cymbron L, Azevedo JT. Heat recovery from Diesel engine exhaust gases for the implementation of a combined cycle. In: INFUB 2008, vol. 8, Portugal, p. 1–9.
[12] Vaja I, Gambarotta A. Internal combustion engine (ICE) bottoming with organic Rankine cycles (ORCs). Energy 2010;35:1084–93.
[13] Bombarda P, Invernizzi CM, Pietra C. Heat recovery from diesel engines: a thermodynamic comparison between Kalina and ORC cycles. Appl Therm Eng 2010;30:212–9.
[14] Gewald D, Schuster A, König N, Spliethoff H. Comparative study of water-steam- and organic-Rankine-cycles as bottoming cycles for heavy-duty diesel engines by means of exergetic and economic analysis. In: ECOS 2010, Lausanne.
[15] Hountalas D, Katsanos C, Kouremenos D, Rogdakis E. Study of available exhaust gas heat recovery technologies for HD diesel engine applications. Int J Altern Propul 2007;1:228–49.
[16] Woodward JB. Evaluation of Brayton and Rankine alternatives for diesel waste heat exploitation. J Eng Gas Turb Power 1994;116:39–45.
[17] Holmes J, Lucas NJ. Optimization of diesel-engine design for combined heat and power. Int J Energy Res 1981;5:61–76.
[18] Windeknecht M. Diplomarbeit: Konzepte zur Nutzung der Ladeluftwärme turboaufgeladener Großdieselmotoren. München; 2010.
[19] NIST National Institute of Standards and Technology. REFPROP: reference fluid thermodynamic and transport properties database; 2010.
[20] STEAG Energy Services GmbH, EBSILON Professional; 2010.
[21] Baehr HD, Kabelac S. Thermodynamik: Grundlagen und technische Anwendungen. Berlin/Heidelberg: Springer; 2009.
[22] Nikulshin V, Wu C, Nikulshina V. Exergy efficiency calculation of energy intensive systems. Exergy – Int J 2002;2:78–86.
[23] Mago PJ, Chamra LM. Exergy analysis of a combined engine-organic Rankine cycle configuration. Proc Inst Mech Eng Part A: J Power Energy 2008;222:761–70.
[24] VDI Wärmeatlas, Springer, Berlin/Heidelberg, 10 ed.; 2006.
[25] Polifke W, Kopitz J. Wärmeübertragung: Grundlagen, analytische und numerische Methoden. Pearson Studium, München/Boston; 2005.
[26] GEA Maschinenkühltechnik GmbH, LLKDREI; 2001.

[27] VDI 2067. Wirtschaftlichkeit gebäudetechnischer Anlagen: Grundlagen der Kostenberechnung; 2000.
[28] Talbi M, Agnew B. Energy recovery from diesel engine exhaust gases for performance enhancement and air conditioning. Appl Therm Eng 2002;22:693–702.
[29] Rakopoulos CD, Dimaratos AM, Giakoumis EG, Rakopoulos DC. Evaluation of the effect of engine, load and turbocharger parameters on transient emissions of diesel engine. Energy Convers Manage 2009;50:2381–93.
[30] Rakopoulos CD, Giakoumis EG, Rakopoulos DC. Cylinder wall temperature effects on the transient performance of a turbocharged diesel engine. Energy Convers Manage 2004;45:2627–38.
[31] Lakew AA, Bolland O. Working fluids for low-temperature heat source. Appl Therm Eng 2010;30:1262–8.
[32] Drescher U, Brüggemann D. Fluid selection for the organic Rankine cycle (ORC) in biomass power and heat plants. Appl Therm Eng 2007;27:223–8.